Journal of Sea Research xxx (2014) xxx–xxx

Contents lists available at ScienceDirect

Journal of Sea Research

journal homepage: www.elsevier.com/locate/seares

Stereological comparison of oocyte recruitment and batch fecundity estimates from paraffin and resin sections using spawning albacore (*Thunnus alalunga*) ovaries as a case study

Sámar Saber [a,b,*], David Macías [a], Josetxu Ortiz de Urbina [a], Olav Sigurd Kjesbu [c,d]

[a] Instituto Español de Oceanografía (IEO), Centro Oceanográfico de Málaga, Puerto pesquero s/n, 29640 Fuengirola, Andalucía, Spain
[b] Departamento de Biología Animal, Universidad de Málaga, 29071 Málaga, Andalucía, Spain
[c] Institute of Marine Research (IMR) and Hjort Centre for Marine Ecosystem Dynamics, P.O. Box 1870 Nordnes, NO 5817 Bergen, Norway
[d] Centre for Ecological and Evolutionary Synthesis (CEES), Department of Biosciences, University of Oslo, P.O. Box 1066 Blindern, NO 0316 Oslo, Norway

ARTICLE INFO

Article history:
Received 15 July 2013
Received in revised form 27 April 2014
Accepted 20 May 2014
Available online xxxx

Keywords:
Shrinkage
Paraffin
Resin
Oocyte Packing Density
Fecundity
Albacore

ABSTRACT

Traditional histological protocols in marine fish reproductive laboratories using paraffin as the embedding medium are now increasingly being replaced with protocols using resin instead. These procedures entail different degrees of tissue shrinkage complicating direct comparisons of measurement results across laboratories or articles. In this work we selected ovaries of spawning Mediterranean albacore (*Thunnus alalunga*) as the subject of our study to address the issue of structural changes, by contrasting values on oocyte recruitment and final batch fecundity given from the same tissue samples in both paraffin and resin. A modern stereological method, the oocyte packing density (OPD) theory, was used supported by initial studies on ovarian tissue sampling and measurement design. Examples of differences in the volume fraction of oocyte stages, free space and connective tissue were found between the embedding media. Mean oocyte diameters were smaller in paraffin than in resin with differences ranging between 0.5% in primary growth and 24.3% in hydration (HYD) stage oocytes. Fresh oocyte measurements showed that oocytes shrank as a consequence of the embedding process, reaching the maximal degree of shrinkage for oocytes in the HYD stage (45.8% in paraffin and 26.5% in resin). In order to assess the effect of oocyte shrinkage on the OPD result, and thereby on relative batch fecundity (F_r), oocyte diameters corrected and uncorrected for shrinkage, were used for estimations. Statistical significant differences were found ($P < 0.05$) between these two approaches in both embedding media. The average F_r was numerically smaller in paraffin compared to resin (86 ± 61 vs. 106 ± 54 oocytes per gram of body mass (mean $\pm$ SD)). For both embedding media statistical significant differences ($P < 0.05$) were seen between F_r results based on either oocytes in the germinal vesicle migration stage or HYD stage. As a valuable adjunct, the present use of the OPD theory made it possible to document that the oocyte recruitment of spawning ovaries of Mediterranean albacore followed the typical pattern of an asynchronous oocyte development and indeterminate fecundity.

1. Introduction

Reproductive classification schemes based on histological techniques represent the most accurate approach (Hunter and Macewicz, 1985). So, histology is frequently used in many marine laboratories for dedicated studies on oocyte development, estimates of fecundity, quantification of ovarian atresia, and sexual maturity of testes, although the latter studies are generally more restricted in numbers. Traditional protocols using paraffin (polyisobutylene mixture) embedding are now increasingly replaced with resin (hydroxyl ethylmethacrylate)-based protocols. This means that new results for a given species using resin might not be directly comparable with those found in earlier reports where the authors used paraffin. One particular relevant issue might be that the various histological procedures entail different degree of tissue shrinkage (Dorph-Petersen et al., 2001). Consequently, data on oocyte size or oocyte size distributions and fecundity estimates for the same species using different methods of preservation, dehydration and embedding techniques should be evaluated cautiously before being contrasted or pooled together. Here we address these types of issues using albacore, *Thunnus alalunga* (Bonnaterre, 1788) as our object of study. As for the other tunas, albacore shows a complicated reproductive style with the production of many egg batches (Schaefer, 2001), i.e. true insights into its numerical production of oocytes require the use of histology in combination with stereology.

* Corresponding author at: Instituto Español de Oceanografía (IEO), Centro Oceanográfico de Málaga, Puerto pesquero s/n, 29640 Fuengirola, Andalucía, Spain. Tel.: +34 952197124; fax: +34 952463808.
E-mail addresses: samar.saber@uma.es (S. Saber), david.macias@ma.ieo.es (D. Macías), urbina@ma.ieo.es (J. Ortiz de Urbina), olav.kjesbu@imr.no (O.S. Kjesbu).

http://dx.doi.org/10.1016/j.seares.2014.05.003
1385-1101/

Stereological methods are in most cases based on histological sections for estimating number and size of different particles. Such studies are widely used in many fields of research, but in particular in medicine including also the issue of shrinkage (Boonstra et al., 1983; Dobrin, 1996; Dorph-Petersen et al., 2001; Johnson et al., 1997; Quester and Schröder, 1997). As for other biological disciplines paraffin and resin are the most commonly used embedding media in fish reproductive studies and different chemicals are also often used to preserve the gonad tissue before the histological processing; however, few of these publications present shrinkage corrections factors. Shrinkage of oocytes may be studied at different levels: (1) from fresh to fixed oocytes, (2) from fixed oocytes to sectioned oocytes, and (3) from fresh to sectioned oocytes. Oocyte shrinkage as a consequence of formalin fixation has been reported to range from 5% to 11% (Kjesbu, 1991; Lowerre-Barbieri and Barbieri, 1993) and from 15% to 22% in the earlier often used Gilson's fluid (DeMartini and Fountain, 1981; Witthames and Walker, 1987). Furthermore, oocyte shrinkage on average was estimated to be 13% and 14% from fixed oocytes to embedded oocytes in paraffin and resin, respectively (Davis, 1982; Korta et al., 2010). However, it has been reported to be up to 48% from fresh to paraffin-embedded oocytes of Baltic cod (*Gadus morhua callarias*) (Kraus et al., 2008) whereas only about 7% from fresh (and thereafter fixed in either formalin or Bouin's fluid) to resin-embedded oocytes of Norwegian coastal cod (*G. morhua*) (Kjesbu et al., 2011). Hence, the use of fixatives and the embedding procedures may cause ovarian tissue to shrink to a greater or lesser extent, and different types of oocytes or structures within the ovary may be affected differently.

Our target of study, the albacore, shows a complicated reproductive style to quantitatively address due to its asynchronous oocyte development and indeterminate fecundity (Schaefer, 2001). Nevertheless, reproductive analyses on these types of multiple spawner species often involve presentations of batch fecundity and oocyte size distributions and are therefore relevant candidates to test the present type of methodological issues. Theoretical oocyte packing density (OPD), a recently developed methodology for accurately estimating the number of oocytes per gram of ovary, has been applied on both determinate and indeterminate fecundity types (Korta et al., 2010; Kurita and Kjesbu, 2009; Schismenou et al., 2012). In these three mentioned studies, indeterminate species were included but different embedding media for the histological analysis were used. Kurita and Kjesbu (2009) emphasized that the OPD result is mainly influenced by oocyte size and volume fraction by studying vitellogenic oocytes embedded in paraffin, whereas Korta et al. (2010) and Schismenou et al. (2012) in their studies on oocyte recruitment used resin and the oocyte shrinkages where found by referring to measurements performed in whole mounts on formalin-fixed oocytes.

Consequently, the main objective of this study was to compare the output from the two most common embedding media used in reproductive-related studies on teleost ovarian tissue, paraffin and resin. To support this objective a case study of Mediterranean albacore was undertaken. The above cited OPD theory was used in order to detail oocyte batch recruitment in spawning individuals and to examine any differences in both the number of stage-specific oocytes per gram and the relative batch fecundity between the two embedding media. In this study fresh oocytes were used to correct oocyte measurements performed in histological sections and, for the first time, oocyte shrinkages resulting from the use of paraffin and resin embedding media were directly compared. Lastly, both uncorrected and corrected oocyte diameters were used to examine how sensitive the numerical estimation of oocytes is to the level of shrinkage.

2. Material and methods

2.1. Outline

In this work 88 albacore females were considered for microscopic maturity classification using in the first instance paraffin as embedding medium.

According to their different developmental stages, oocytes were classified using the terminology of Brown-Peterson et al. (2011), namely: primary growth, cortical alveolar, primary vitellogenic, secondary vitellogenic, tertiary vitellogenic, germinal vesicle migration and hydration stages. However, as not only oocytes in the latter two advanced developmental stages (along with a limited amount of atresia) but also the presence of postovulatory follicles (POFs) reflects actively spawning tunas (Chen et al., 2010; Farley et al., 2013; Schaefer, 1998), the adopted terminology used for the ovary reproductive phases had to be adjusted accordingly. The background being that POFs in this category of fishes, spawning typically in warm waters, are quickly resorbed, i.e. within c. 24 h (Farley et al., 2013; Hunter et al., 1986; McPherson, 1991; Schaefer, 1996). Additionally, these ovaries were classified in four subphases according to the most advanced oocyte stage present in the ovary.

Based on this histological screening a sub-group of ovaries was selected for the main stereological study using both resin and paraffin (Fig. 1). Prior to initiating this main study, a few out of these ovaries were included in a pilot study to address relevant accuracy and precision issues (Fig. 2). An additional sample of ovaries was also collected after the main sampling program to estimate ovarian specific gravity and oocyte shrinkage (Fig. 1) to fulfill data requirements to properly apply the oocyte packing density formula (see below). The total number of 88 ovaries was randomly selected from fish caught in fishing tournaments and by longline vessels targeting spawning *T. alalunga* in the western Mediterranean Sea in July 2007, 2008 and 2010. Each specimen was weighed to the nearest 0.1 kg (body mass [BM]: 4.0–12.3 kg) and measured for fork length (FL: 58–86.5 cm). Ovaries were removed and gonad mass (GM) measured to the nearest g. Assuming no systematic differences in ovarian homogeneity (structural characteristics), either throughout the whole ovary including between the two ovarian lobes (Otsu and Uchida, 1959; Stéquert and Ramcharrun, 1995), a full cross-section (2–3 cm wide) from the central part of one of the lobes was fixed in Bouin's fluid for 4 h and then preserved in 70% ethanol. The fresh ovaries selected for ovarian density and oocyte diameter shrinkage estimations were collected from a fishing tournament (FL: 59–83.5 cm) in July 2011 at the same location as previously. In the same way, these ovaries were histologically classified using paraffin as embedding medium.

2.2. Histology and microscopical classification of ovaries used for further selection

Based on an earlier study on albacore (Otsu and Uchida, 1959) indicating transversal structural differences in the ovary affecting oocyte distribution, a sub-sample was taken from each ovary including the area from the *tunica albuginea* to the ovarian lumen. These representative sub-samples were then dehydrated through increasing concentrations of ethanol series, cleared with n-butanol and embedded in Paraplast Plus®, i.e. paraffin. Histological sections of 10 μm were cut using a microtome and stained with Mallory's trichrome stain. In all of the ovaries considered for microscopic examination (including those collected in 2011) POFs and a few atretic follicles were detected. As a result, all females were classified as spawning, more specifically, as actively spawning; the ovaries were split into one of four subphases according to the most advanced oocyte stage present (Table 1). Hence oocyte stages were described according to their histological characteristics (Table 1).

A total of 22 ovaries (15 from the main study and 7 from the shrinkage study) (Fig. 1) in AVT, MG and HY subphases (see Table 1 for abbreviations) were randomly selected for subsequent embedding in resin. A representative sub-sample of each ovary was polymerized into one or two (when the tissue sub-samples were large) blocks using conventional techniques with Technovit® 7100 as embedding medium, sectioned at 4 μm and stained with 2% toluidine blue and 1% sodium tetraborate (borax). In line with the practice used during the pilot study (Fig. 2),

Please cite this article as: Saber, S., et al., Stereological comparison of oocyte recruitment and batch fecundity estimates from paraffin and resin sections using spawning albac..., J. Sea Res. (2014), http://dx.doi.org/10.1016/j.seares.2014.05.003

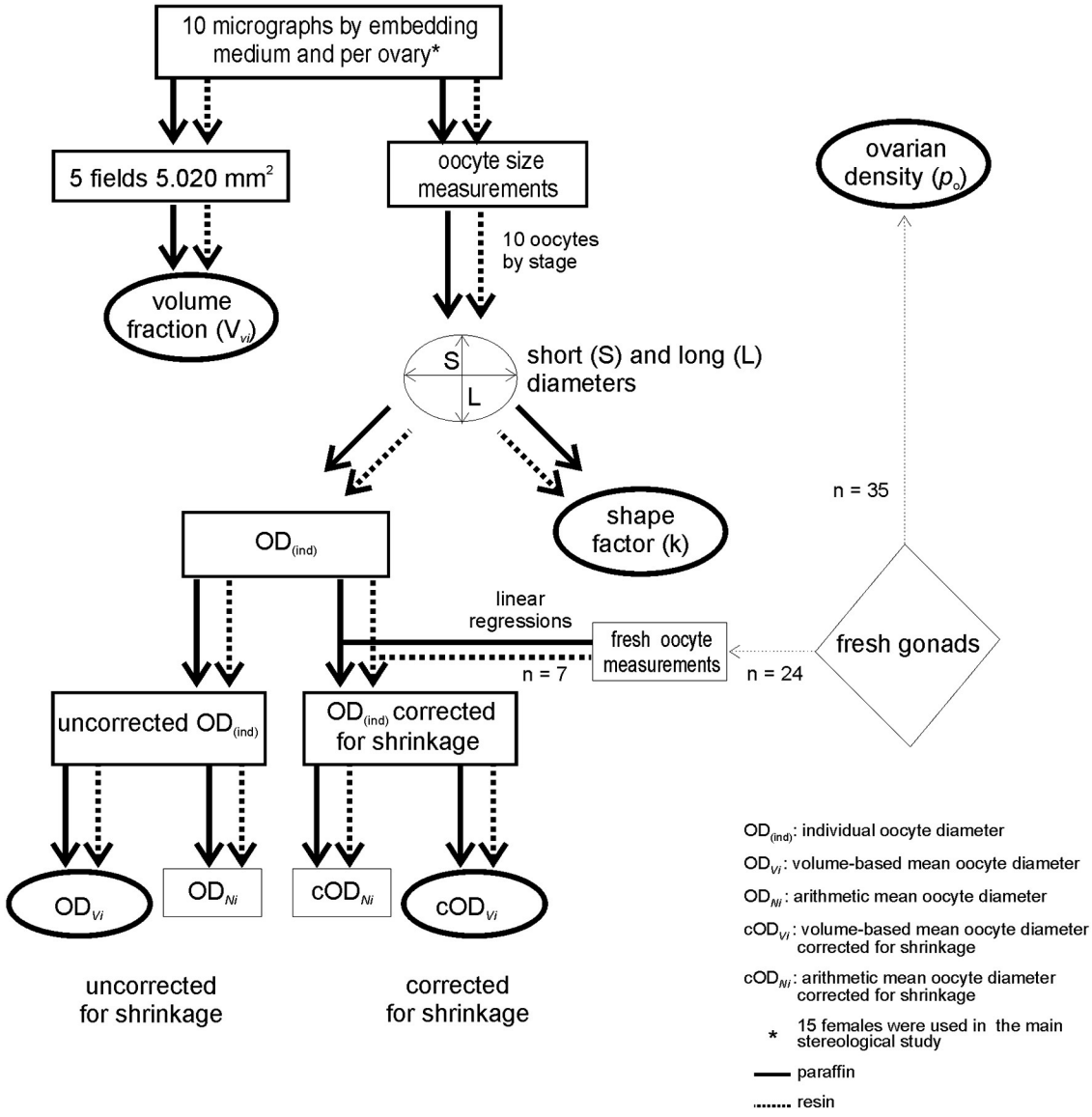

Fig. 1. Overview of the main study carried out with 15 of the 88 females considered for microscopic maturity ovary classification. For details, see the description in Material and methods.

for each ovary in the main study ten micrographs of both paraffin and resin histological sections were taken with a resolution of 0.846 pixels/μm with a Nikon photomicroscope and stored for further image analysis depending of the outcome of the pilot study guidelines. Several histological sections (from two to four sections depending on the section size) separated 1000 μm apart were photographed considering the whole cross section in a uniform random fashion, that is, from the ovarian wall to the ovarian lumen in each section.

2.3. Theoretical oocyte packing density (OPD)

The oocyte packing density (OPD) was estimated theoretically for each stage *i* oocyte (i.e., types of developing oocytes, see below), using the above paraffin and resin sections, according to the formula of Korta et al. (2010) and Schismenou et al. (2012), originally developed by Kurita and Kjesbu (2009):

$$\log(\mathrm{OPD}_i) = \log\left[V_{Vi} \times (1/\rho_o) \times \left\{(1+k)^3/(8\times k)\right\}\right] + 12.28 - 3 \times \log(\mathrm{OD}_{Vi}) \quad (1)$$

were,

- OPD_i refers to the number of stage *i* oocytes per gram of ovary, g^{-1};
- V_{Vi} is the volume fraction of stage *i* oocytes;
- ρ_o is the ovarian density, g cm^{-3};
- k is the shape factor; the mean ratio of short (S) and long (L) diameters of individual stage *i* oocytes;
- OD_{Vi} is the volume-based mean oocyte diameter of stage *i* oocytes, μm (given from mean oocyte volume).

The sum of OPD_i of all stage *i* oocytes in the ovary was the total number of oocytes per gram of ovary (OPD). In addition, in order to get insight into the effect of oocyte shrinkage on relative batch fecundity estimates, OPD_i was calculated using estimates of OD_{Vi} and cOD_{Vi} (see Section 2.3.4.) calculated from both individual oocyte diameter ($\mathrm{OD}_{(ind)}$), uncorrected and corrected (here abbreviated as c in front of the term) for shrinkage, respectively.

The oocytes were grouped into five stages per gonad subphase: (1) primary growth (PG) in an early phase: homogeneous basophilic cytoplasm with no cytoplasmic inclusions; (2) cortical alveolar (CA): small

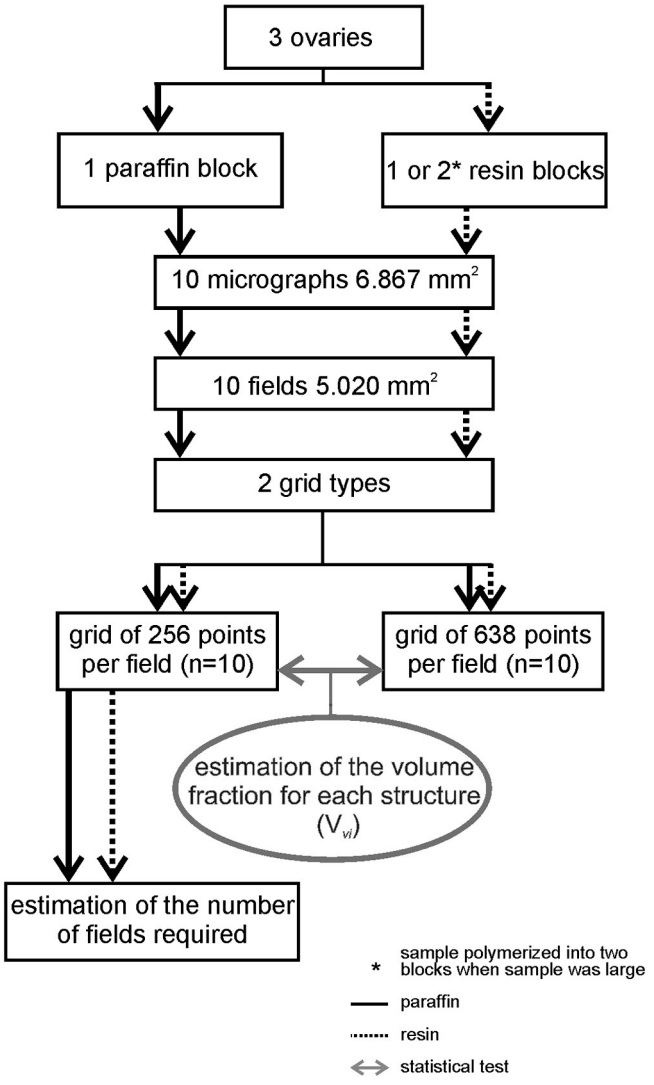

Fig. 2. Overview of the pilot study carried out with 3 of the 15 ovaries included in the main study.

lipid droplets in the cytoplasm but still no yolk granules; (3) primary vitellogenic (Vtg1): yolk granules in the periphery of the cytoplasm and lipid droplets occupy more of the cytoplasmic area than the yolk granules; (4) secondary vitellogenic (Vtg2) (for definition see Table 1) and (5), depending on the most advanced oocyte stage present in the ovary, the fifth oocyte stage was either tertiary vitellogenic (Vtg3), germinal vesicle migration (GVM) or hydration (HYD) stages (for definitions see Table 1).

2.3.1. Volume fraction (V_V)

The volume fraction was estimated for every oocyte stage *i* and for 'others' (V_{Vi}), which in the latter respect included connective tissue (the relatively few points hitting blood capillaries were also for simplicity included in the connective tissue volume fraction), postovulatory follicles, atretic follicles, lost oocytes (space that assumingly had been occupied by oocytes), and free space (extracellular space) in paraffin and resin histological sections following the Delesse principle (Howard and Reed, 2010). This principle states that the fractional cross-sectional area of a component in the tissue under examination is proportional to its fractional volume. The estimation of volume fraction was calculated using the software ImageJ (http://rsb.info.nih.gov/ij/) for each structure as the ratio between the grid points hitting stage *i* oocytes or 'others' and the total points hitting the sectioned tissue: V_{Vi} = number of hits for stage *i* oocyte or 'others' / (total of grid points − number of hits hitting outside the sectioned tissue), so that, the sum of all estimated volume fractions in each field added up to 1.

The three ovaries in the pilot study (Fig. 2), being in AVT, MG and HY subphases, were specifically used to clarify not only to which degree the number of grid points per field but also how the number of fields used in the analysis influence the accuracy of individual V_{Vi} estimates. Hence, we aimed to locate reasonable trade-offs between work load and data quality prior to undertaking the main study. For each of the selected ovaries in question volume fraction was estimated using two grid types, 256 points versus 638 points, but of the same size (Fig. 2) and with a constant number of fields (10), i.e., a total of 40 counting fields per ovary were used for estimating volume fraction: 20 fields (10 micrographs from paraffin sections and 10 from resin sections) per each of the two grid types. No significant differences ($P > 0.05$, ANOVA) were found in observed volume fraction between the grid types. The 256 grid type was therefore the logical choice due to the less work involved in getting these data (Fig. 2). Regarding the number of fields required, the estimates of volume fraction of stage *i* oocytes (grid of 256 points per field) by embedding medium and per gonad subphase were used to compute the coefficient of variation (CE) of each oocyte stage by using five counting fields out of the 10 available (Korta et al., 2010), i.e., to test if this restricted number of field would be sufficient for the present purpose. The estimated CE for PG, CA, Vtg1 and Vtg2 stage oocytes ranged between 0.09 and 0.34 and, for Vtg3, GVM and HYD stage oocytes between 0.05 and 0.12. Taking into account that the estimated CE of the last most advanced group of oocytes (MAGO) in each ovary did not exceed 0.12, it was decided to go for five counting fields per embedding medium (Fig. 1) in the following procedure. The five counting fields (micrographs) out of the 10 available per ovary and embedding medium were randomly selected so that different parts of each whole cross section had an equal chance of being represented. Thus, altogether 10 counting fields per ovary (five from paraffin and five from resin) were used for volume fraction estimations of each stage *i* oocyte and for 'others'. This practice was analogous to Korta et al. (2010) and Schismenou et al. (2012), although these authors used only one embedding medium (resin) and did not test for the influence of grid type resolution.

2.3.2. Oocyte size measurements from paraffin and resin slides

From the ten micrographs per embedding medium, ten oocytes of each stage *i* oocyte present in the ovary were measured using ImageJ software (http://rsb.info.nih.gov/ij) and the plugin ObjectJ (http://simon.bio.uva.nl/objectj/). Only oocytes sectioned through the nucleus (from PG to GVM stages) were considered for measurements of L and S diameters, calculating thereafter individual oocyte diameter ($OD_{(ind)} = (L + S)\ 2$), L / S ratio, arithmetic mean oocyte diameter (OD_{Ni}) and volume-based mean oocyte diameter (OD_{Vi}) (Korta et al., 2010; Kurita and Kjesbu, 2009; Schismenou et al., 2012) (Fig. 1):

$$OD_{Ni} = \sum_{j=i}^{n_i} \frac{OD_{(ind)i,j}}{n_i} \tag{2}$$

$$OD_{Vi} = \left[\sum_{j=i}^{n_i} \left(\frac{\left(OD_{(ind)i,j}\right)^3}{n_i} \right) \right]^{\frac{1}{3}}. \tag{3}$$

In the case of PG stage, only oocytes with $OD_{(ind)} > 100$ μm were considered.

2.3.3. Ovarian density (ρ_o)

The ovary volume of the samples collected in 2011 (Fig. 1) was measured using Scherle's method (Scherle, 1970), that is, by the weight of

Table 1
Spawning ovary subphases defined for spawning female Mediterranean albacore (*Thunnus alalunga*) based on the most advanced group of oocytes (MAGO) present in the ovary.

Gonad subphases	n[a]	n[b]	MAGO. Histological characteristics
Medium vitellogenic (MVT)	21	5	Secondary vitellogenic (Vtg2) stage: Yolk granules and lipid droplets are spread throughout the cytoplasm.
Advanced vitellogenic (AVT)	33	19	Tertiary vitellogenic (Vtg3) stage: Larger yolk granules than that of MVTO. Lipid droplets fuse and are distributed around the nucleus.
Migratory nucleus (MG)	28	10	Germinal vesicle migration (GVM) stage: Lipid droplets fuse into 1–3 large droplets. Migration of the nucleus toward the animal pole. In a later phase, yolk granules fuse progressively.
Hydrated (HY)	6	1	Hydration (HYD) stage: The nucleus has disintegrated. All yolk granules fuse into a homogeneous yolk mass and the oocyte increases in size due to hydration. The oocyte is still surrounded by the follicle layer, i.e. ovulation has yet not taken place.
Total females	88	35	

[a] Number of ovaries collected in 2007, 2008, and 2010.
[b] Number of ovaries collected in 2011.

physiological seawater ($\rho = 1.0107$ g cm^{-3}) displaced. Ovarian density was then calculated from the weight and volume of each ovary (see Results section). As immature and developing ovarian phases (Brown-Peterson et al., 2011) were not detected in this study, a sensitive analysis was performed in order to observe the effects of ovarian density on OPD_i estimations for PG, CA and Vtg1 stage oocytes. The considered ovarian densities to carry out the sensitive analysis were: 1.056–1.065 g cm^{-3} for PG and CA stages and 1.070–1.079 g cm^{-3} for Vtg1 stage, based on a literature review (see Korta et al., 2010 and references therein; Schismenou et al., 2012). The analysis showed that when OPD_i was estimated using low values of ρ_o, OPD_i increased, and contrarily, when the OPD_i was estimated using higher values of ρ_o, OPD_i decreased, although these differences in OPD_i were very small within the assumingly realistic range in ρ_o (Table 2). Hence, the ovarian densities collated by Korta et al. (2010) for these oocyte stages were adopted in the further calculations of OPD_i.

2.3.4. Fresh oocyte measurements for correcting oocyte shrinkage

In order to obtain accurate estimates of OPD_i, oocyte diameters measured from histological sections were corrected for shrinkage. A slice from the central part of the right ovarian lobe of 24 fresh gonads out of the 35 collected for ovarian density estimations was first measured for fresh oocyte size (Fig. 1) and thereafter fixed and preserved as previously described. Small pieces of tissue were slightly stirred with a few drops of isotonic water, spread out on a petri dish and, if needed, a needle was gently used under a stereomicroscope (Leica) to manually separate clumps of oocytes or oocytes attached to connective tissue. These fresh oocytes were then photographed with a resolution of 0.982 pixels/μm. Months later, the gonad subphases were histologically confirmed: advanced vitellogenic (n = 15), migratory nucleus (n = 8) and hydrated (n = 1). Then, a subset of seven ovaries (Fig. 1) of advanced vitellogenic (n = 3), migratory nucleus (n = 3) and hydrated (n = 1) gonad subphases were selected for oocyte shrinkage corrections, and the histological paraffin and resin sections were photographed with a resolution of 0.630 pixels/μm using a Nikon photomicroscope. From the micrographs, ten fresh oocytes and twenty sectioned oocytes (ten embedded in paraffin and ten in resin) of the MAGO present in each ovary, i.e. Vtg3, GVM and HYD stages, were measured as previously described. For each separate embedding medium the measured mean diameters of fresh oocytes (OD_{fresh}) were regressed onto the mean diameters of oocytes measured in histological sections. Hence, individual oocyte diameters ($OD_{(ind)}$) in the main study could be corrected for shrinkage using the resulting equations, and in turn these corrected measurements were used to estimate both the mean oocyte diameter (cOD_{Ni}) and the volume-based mean oocyte diameter corrected for shrinkage (cOD_{Vi}).

2.3.5. Estimation of batch fecundity

Batch fecundity was defined as the number of oocytes released in a single spawning event, i.e. should be considered equal to be the number of oocytes in the germinal vesicle migration (GVM) or hydration (HYD) stages in the ovary (Hunter et al., 1985). Consequently, the estimated number of oocytes in the GVM and HYD stages per gram of ovary, OPD_{GVM} and OPD_{HYD}, respectively, were multiplied with gonad weight. Relative batch fecundity (F_r) was calculated by dividing the batch fecundity by the body mass of the fish.

2.4. Statistical analyses

One-way analysis of variance (ANOVA) (Zar, 1984) was performed for testing differences in volume fraction between grids. For each gonad subphase a paired-sample *t*-test (Zar, 1984) was conducted to test for differences in the volume fraction of each stage *i* oocyte, connective tissue and free space associated with the embedding medium. When the underlying assumptions were not met, non-parametric tests (Wilcoxon and Kruskal–Wallis) were performed (Zar, 1984). To test for potential differences in stage *i* oocyte size measurements between the two embedding media a paired-sample *t*-test was again applied to the data recorded for each gonad subphase. Here we also used the same non-parametric statistics as above when this was required. The same type of statistical analyses was applied to test for differences in OPD_i, obtained by using either $OD_{(ind)}$ uncorrected and corrected for shrinkage, and between the two embedding media. ANOVA followed by Tukey's post hoc test were included to test for significant differences between embedding media in terms of relative batch fecundity obtained by using either 1) uncorrected or corrected $OD_{(ind)}$, and 2) GVM or HYD stage oocytes. All statistical analyses were conducted using R statistical software (R Core Team, 2012). A 5% significance level ($\alpha = 0.05$) was adopted in all tests.

Table 2
Estimates of oocyte packing density (OPD_i) of Mediterranean albacore (*Thunnus alalunga*) using optional values of ovarian density (ρ_o) for the oocyte stages: primary growth (PG), cortical alveolar (CA) and primary vitellogenic (Vtg1) oocyte stages.

Embedding medium	Oocyte stage	ρ_o[a] (g cm^{-3})	OPD_i[b] (g^{-1})	ρ_o[a] (g cm^{-3})	OPD_i[b] (g^{-1})	Differences (%)
Resin	PG	1.056	40,477	1.065	40,135	342 (0.85)
Resin	CA	1.056	2061	1.065	2043	17 (0.85)
Resin	Vtg1	1.070	2143	1.079	2125	18 (0.83)
Paraffin	PG	1.056	40,708	1.065	40,364	344 (0.85)
Paraffin	CA	1.056	2879	1.065	2854	24 (0.85)
Paraffin	Vtg1	1.070	2422	1.079	2402	20 (0.83)

[a] Ovarian density values considered to carry out the sensitive analysis came from literature review.
[b] Oocyte packing density results obtained by using $OD_{(ind)}$ corrected for shrinkage.

Please cite this article as: Saber, S., et al., Stereological comparison of oocyte recruitment and batch fecundity estimates from paraffin and resin sections using spawning albac..., J. Sea Res. (2014), http://dx.doi.org/10.1016/j.seares.2014.05.003

3. Results

3.1. Volume fraction

In general, the volume fraction of oocytes (V_{Vi}) increased when the volume-based mean oocyte diameter increased in all ovarian subphases with the exception of V_{Vi} of PG stage oocytes (Fig. 3). The mean volume fraction of PG stage oocytes was in every case greater than the mean volume fraction of CA and Vtg1 stage oocytes (Table 3). Diameter-specific V_{Vi} of Vtg3 stage oocytes was higher than the corresponding result for oocytes in the GVM and HYD stages (Fig. 3), although some Vtg2 might have been included among the Vtg3 stage in situations when the nucleus was not seen in the histological section. Generally, the volume fraction of "lost oocytes", postovulatory follicles and atresia was small in both resin and paraffin embedding media; the maximum values were 2.6%, 0.8% and 0.2%, respectively (Table 3). All ovaries examined presented POFs, and their volume fraction was lower at the HY gonad subphase (≤0.2%) than at the AVT and MG gonad subphases (0.7–0.8%) (Table 3).

When comparing the embedding media, estimates of volume fraction of the earlier oocyte stages (PG, CA and Vtg1) were generally higher in paraffin than in resin (Table 3). In contrast, volume fraction of the later oocyte stages (Vtg2, Vtg3, GVM and HYD) was lower (Table 3). Statistically significant differences in volume fraction of some oocyte *i* stages were found between paraffin and resin: 1) in the V_{Vi} of CA stages ($P < 0.05$), 2) in the V_{Vi} of Vtg2 stage ($P < 0.05$), but only when the gonad subphase was characterized as hydrated and, 3) in the V_{Vi} of the most advanced oocyte stages at all gonad subphases ($P < 0.001$). So clearly V_{Vi} of the most advanced oocyte stages at all gonad subphases are lower in paraffin (Table 3). This difference was in particular high for oocytes in the HYD stage: the volume fractions were 43 ± 9% and 27 ± 6% (mean ± SD) in resin and paraffin, respectively. Therefore these reductions in volume fraction in paraffin could be expected to be compensated by increasing volume fraction of free space (extracellular space) at all gonad subphases (Fig. 4). In general, there was an upward trend in volume fraction of free space, from 7% to 12% in resin and from to 17% to 29% in paraffin, as the gonad subphase progressed (Table 3). These noted differences in free space volume fraction between embedding media were statistically confirmed ($P < 0.001$). Estimates of connective tissue were higher in resin than in paraffin but statistical differences were only found in AVT and MG gonad subphases ($P < 0.01$).

3.2. Oocyte size

A total of 1500 stage *i* oocytes (750 in each embedding medium) were measured in histological sections (Fig. 4). Mean oocyte diameters (OD_{Ni}) were lower in paraffin than in resin, with differences ranging between 0.5% (PG) to 24% (HYD) (Table 4). The diameter range of the oocytes in the HYD stage embedded in paraffin almost coincided with the corresponding diameter range for the GVM stage oocytes (Table 4). Significant differences in mean oocyte diameter of all stage *i* oocytes between the two embedding media were found ($P < 0.05$), except in PG stage oocytes in AVT and MG gonad subphases ($P > 0.05$).

3.3. Ovarian density

The estimated mean values of ovarian density (ρ_o) were 1.069 g cm^{-3} for MVT gonad subphase (n = 5); 1.072 g cm^{-3} for AVT gonad subphase (n = 19) and 1.064 g cm^{-3} for MG/HY gonad subphases (n = 11; weighted average), i.e. the corresponding values for 1 / ρ_o were 0.935, 0.933 and 0.940 cm^3 g^{-1}, respectively. The adopted values of ovarian densities for PG and CA oocyte stages were 1.061 g cm^{-3}, while 1.072 g cm^{-3} for Vtg1 stage oocyte, i.e. 1 / ρ_o in the OPD estimations were here set to 0.943 cm^3 g^{-1} for PG and CA stage oocytes, and to 0.933 cm^3 g^{-1} for Vtg1 oocyte stage.

3.4. Oocyte shrinkage

All stage *i* oocytes shrank during tissue processing, but they shrank more in paraffin (Table 5 and Fig. 4). Mean HYD stage oocyte diameter decreased more than Vtg3 and GVM stage oocyte diameters in both embedding media. The relative degree of difference in shrinkage between paraffin and resin was not stable across all oocyte stages (Table 5). These patterns were in accordance with those found for Vtg3, GVM and HYD stage oocytes in the main study (see Table 4). Based on the differences in mean diameter between fresh and embedded oocytes, it was clear that exposure to either embedding protocols caused oocyte shrinkage. In addition, the observations suggested a higher shrinkage rate for oocytes in the HYD stage. Then, in order to accurately correct for oocyte shrinkage OD_{fresh} was regressed on mean diameter of oocytes from histological sections, studying each embedding medium separately and oocytes in the Vtg3 + GVM and HYD stages. The established regression lines used to correct oocyte shrinkage were:

$$OD_{fresh} = 24.81 + 1.298 \times OD_{paraffin} \text{(for paraffin PG–GVM stage oocytes)} \quad (4)$$

$$OD_{fresh} = 265.11 + 1.298 \times OD_{paraffin} \text{(for paraffin HYD stage oocytes)} \quad (5)$$

$$OD_{fresh} = 43.03 + 1.129 \times OD_{resin} \text{(for resin PG–GVM stage oocytes)} \quad (6)$$

$$OD_{fresh} = 152.71 + 1.129 \times OD_{resin} \text{(for resin HYD stage oocytes)} \quad (7)$$

3.5. Arithmetic and volume-based oocyte size

The absolute differences between the volume-based mean oocyte diameter (cOD_{Vi}) and the arithmetic mean oocyte diameter (cOD_{Ni}) corrected for shrinkage were very small for all stage *i* oocytes, i.e. from 0.08 to 3.82 μm for oocytes measured in resin slides and from 0.13 to 3.02 μm for oocytes measured in paraffin slides; this issue was considered to be of negligible importance.

3.6. Stage-specific oocyte packing density

The estimated number of PG stage oocytes per gram of ovary (OPD_{PG}) was very high in all gonad subphases and for both embedding media.

Generally, the total number of oocytes per gram of ovary in the case of cOD_{Vi} (based on $OD_{(ind)}$ corrected for shrinkage) was one third of that for OD_{Vi} (based on $OD_{(ind)}$ uncorrected for shrinkage) (Table 6). In addition, comparing OD_{Vi}-based OPD_i in paraffin with those in resin, paraffin showed consistently higher values than resin, especially for oocytes in the HYD stage. Statistically significant differences in the estimations of OPD_i were found when using OD_{Vi} and cOD_{Vi} for all oocyte stages and for both embedding media ($P < 0.05$).

When comparing OPD_i results after proper oocyte shrinkage corrections, i.e., using cOD_{Vi}, between the two embedding media, OPD_i estimates in paraffin for the smallest oocytes (from PG to Vtg1 stages) were in general higher than in resin. In contrast, the estimated number per gram of ovary of Vtg2 stage oocyte and of the most advanced

Please cite this article as: Saber, S., et al., Stereological comparison of oocyte recruitment and batch fecundity estimates from paraffin and resin sections using spawning albac..., J. Sea Res. (2014), http://dx.doi.org/10.1016/j.seares.2014.05.003

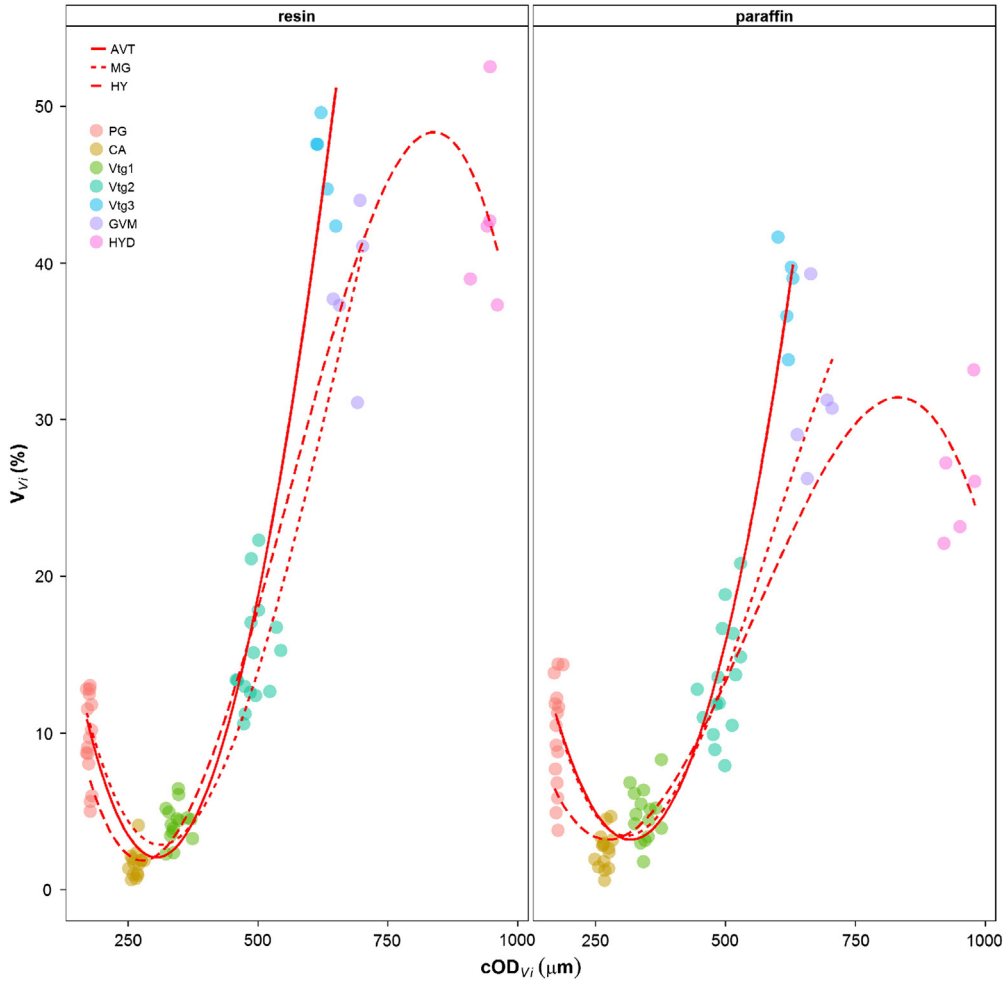

Fig. 3. Oocyte volume fraction (V_{Vi}) at different gonad subphases in spawning capable albacore (*Thunnus alalunga*): advanced vitellogenic (AVT), migratory nucleus (MG) and, hydrated (HY) gonad subphases plotted against volume-based mean oocyte diameter (cOD_{Vi}) (line is fitted by 3rd-order polynomial regression). Oocyte stages: PG = primary growth; CA = cortical alveolar; Vtg1 = primary vitellogenic; Vtg2 = secondary vitellogenic; Vtg3 = tertiary vitellogenic; GVM = germinal vesicle migration and HYD = hydration.

stage oocytes across gonad subphases in paraffin were lower than in resin. However, only significant differences in OPD_i estimates for CA stage (only at AVT gonad subphase) ($P < 0.05$) and for HYD stage oocytes ($P < 0.01$) between the two embedding media were found. Furthermore, total number of oocytes per gram of ovary (total OPD) decreased as the gonad progressed through development but with no evidence of any statistical difference between resin and paraffin in this respect ($P > 0.05$) (Table 6).

Table 3
Estimates of mean volume fraction for every oocyte stage *i* present in each gonad subphase and for "others" (see main text) in both paraffin and resin embedding media in the Mediterranean albacore (*Thunnus alalunga*) ovaries. Gonad subphases: Advanced vitellogenic (AVT), migratory nucleus (MG) and hydrated (HY). Oocyte stages: PG = primary growth; CA = cortical alveolar; Vtg1 = primary vitellogenic; Vtg2 = secondary vitellogenic; Vtg3 = tertiary vitellogenic; GVM = germinal vesicle migration and HYD = hydration.

	Resin			Paraffin		
Volume fraction	Gonad subphase			Gonad subphase		
Structure	AVT	MG	HY	AVT	MG	HY
Oocyte stages:						
– PG	0.108	0.112	0.077	0.115	0.113	0.073
– CA	0.018*	0.025*	0.012*	0.025*	0.036*	0.018*
– Vtg1	0.045	0.051	0.035	0.055	0.059	0.036
– Vtg2	0.125	0.140	0.185*	0.110	0.121	0.157*
– Vtg3	0.457*			0.379*		
– GVM		0.381*			0.305*	
– HYD			0.427*			0.275*
Connective tissue:	0.169*	0.180*	0.142	0.130*	0.136*	0.126
Free space:	0.071*	0.094*	0.119*	0.172*	0.198*	0.294*
Lost oocyte:	–	0.008	–	0.005	0.026	0.018
POFs:	0.007	0.008	0.001	0.007	0.007	0.002
Atresia:	–	0	0.002	0.001	0	0.002

* Indicates values significantly different between resin and paraffin embedded samples.

Please cite this article as: Saber, S., et al., Stereological comparison of oocyte recruitment and batch fecundity estimates from paraffin and resin sections using spawning albac..., J. Sea Res. (2014), http://dx.doi.org/10.1016/j.seares.2014.05.003

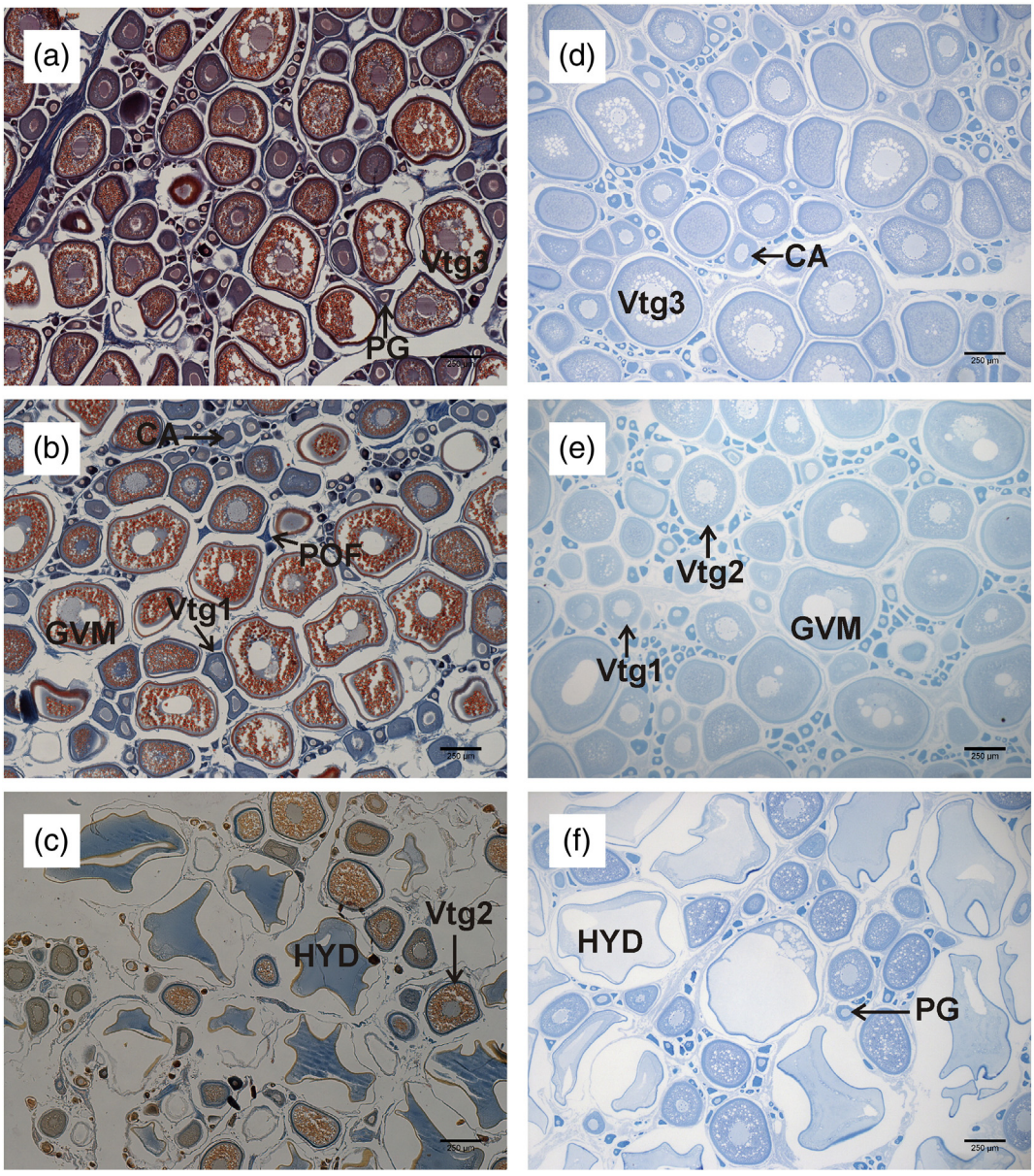

Fig. 4. Micrographs of ovarian tissue embedded in paraffin (a, b and c) and resin (d, e and f) at different gonad subphases in spawning capable albacore (*Thunnus alalunga*): advanced vitellogenic (a and d), migratory nucleus (b and e) and hydrated gonad subphases (c and f). Other abbreviations are as follows: PG = primary growth; CA = cortical alveolar; Vtg1 = primary vitellogenic; Vtg2 = secondary vitellogenic; Vtg3 = tertiary vitellogenic; GVM = germinal vesicle migration and HYD = hydration stage oocytes; POF = postovulatory follicle. Paraffin histological sections were stained with Mallory's trichrome and resin histological sections with 2% toluidine blue and 1% sodium tetraborate (borax). Scale bar = 250 μm.

3.7. Batch fecundity

Of the ovaries used in the main study, ten contained oocytes in the hydration (with no new POFs) or germinal vesicle migration stages, i.e. considered suitable for batch fecundity estimation. Batch fecundity estimates of the ten females ranged from 0.24 million oocytes to 1.24 million oocytes (0.72 ± 0.28 million oocytes (mean ± SD)) for resin and from 0.14 to 1.27 million oocytes (0.56 ± 0.30 million oocytes (mean ± SD)) for paraffin. So in this particular case on average altogether about 160,000 more oocytes were said to present in resin- than in paraffin-based protocols. These estimations differed markedly from those based on oocyte diameters uncorrected for shrinkage, being two times higher in resin and three and a half times higher in paraffin (Table 7).

The relative batch fecundity of the ten females ranged from 32 to 221 oocytes per gram of body mass (mean ± SD: 106 ± 54 g^{-1}) for resin and from 19 to 226 oocytes per gram of body mass (mean ± SD: 86 ± 61 g^{-1}) for paraffin. In the same way as for batch fecundity, comparing results of F_r using cOD_{Vi} with those using uncorrected shrinkage estimations, the latter overestimated relative batch fecundity (Table 7); statistical significant differences were apparent ($P < 0.05$). However, when comparing F_r after shrinkage corrections between the two embedding media there were no differences in F_r ($P > 0.05$).

Finally, we undertook two direct comparisons of mean relative batch fecundity after shrinkage corrections using the five ovaries in the migratory nucleus subphase and the five in the hydrated subphase. The first comparison was between embedding media for the same oocyte stages and the second comparison was between the GVM and HYD stage

Please cite this article as: Saber, S., et al., Stereological comparison of oocyte recruitment and batch fecundity estimates from paraffin and resin sections using spawning albac..., J. Sea Res. (2014), http://dx.doi.org/10.1016/j.seares.2014.05.003

Table 4
Mean oocyte diameter (OD_{Ni}) and diameter ranges (both pooled across gonad subphases) for each stage *i* oocytes in Mediterranean albacore (*Thunnus alalunga*) ovaries. Oocyte stages: PG = primary growth; CA = cortical alveolar; Vtg1 = primary vitellogenic; Vtg2 = secondary vitellogenic; Vtg3 = tertiary vitellogenic; GVM = germinal vesicle migration and HYD = hydration. Oocyte diameters of the oocyte stages from PG to GVM were measured for those oocytes sectioned through the nucleus (with visible nuclei) in both paraffin and resin histological sections. The differences between the two measurements (percent in parenthesis) are given.

		Diameter ranges (μm)		OD_{Ni} ± SD (μm)		
Oocyte stage	n	Resin	Paraffin	Resin	Paraffin	Difference (%)[a]
PG	150	107–137	106–136	117 ± 7	116 ± 6	1 (0.5)
CA	150	162–239	159–219	197 ± 15	187 ± 14	10 (5.0)
Vtg1	150	221–324	207–319	265 ± 23	246 ± 20	19 (7.0)
Vtg2	150	324–483	300–434	397 ± 32	361 ± 26	36 (9.2)
Vtg3	50	465–594	412–503	516 ± 25	458 ± 19	59 (11.3)
GVM	50	498–619	454–555	562 ± 28	498 ± 25	64 (11.4)
HYD	50	592–778	454–602	696 ± 44	527 ± 37	169 (24.3)

n, number of oocytes measured per embedding medium.
[a] Differences in mean oocyte diameter (OD_{Ni}) between the two embedding media (paraffin vs. resin) expressed as percentages (Z), according to the formula: $Z = 100 \times (OD_{resin} - OD_{paraffin}) / OD_{resin}$.

oocytes in the two different embedding media. When we compared the embedding media, of the five ovaries in the migratory nucleus subphase (131 ± 57 vs. 147 ± 43 oocytes per gram of body mass in paraffin and in resin, respectively) and the five ovaries in the hydrated subphase (42 ± 17 vs. 65 ± 20 oocytes per gram of body mass in paraffin and in resin, respectively), the estimations of mean F_r were numerically lower in paraffin than in resin but not significantly ($P > 0.05$). However, in the comparison between GVM and HYD oocyte stages there were significant differences in both embedding media ($P < 0.05$). For paraffin 131 ± 57 GVM stage oocytes against 42 ± 17 HYD stage oocytes per gram of body mass, and for resin 147 ± 43 GVM stage oocytes against 65 ± 20 HYD stage oocytes per gram of body mass.

4. Discussion

It is well known that the process of fixation and histological processing causes the tissue under consideration to shrink. Consequently, any estimates of oocyte size and numbers should be considered in light of the method used, in particular when contrasting values across different protocols. Oocyte shrinkage has been reported to be rapid in the first five days post-fixation and thereafter minor but still happening in Gilson's fluid, i.e. Gilson's fluid should not be considered as a preservative as such as its role is to break down connective tissue (Witthames and Walker, 1987). In true preservatives, such as formalin, no significant differences in oocyte size have been found between after 3–4 months and after 6–7 months (Lowerre-Barbieri and Barbieri, 1993). All the samples used in the present study were fixed in Bouin's fluid and preserved in 70% ethanol for at least three months prior to embedding. Then, it was assumed that the oocyte shrinkage as a consequence of preservation time of the ovarian samples did not vary among all of the samples examined. An alternative to using embedded oocytes when undertaking oocyte measurements is the use of frozen ovaries, but it has been observed that the mean diameter of oocytes of frozen ovaries are significantly smaller than those preserved in formalin (Ramon and Bartoo, 1997). Moreover, frozen ovaries are usually excluded for fecundity estimations especially when the oocytes are small and liable to cell disruption, but technical measures, such as storing them in sucrose, do exist for some species (Kjesbu and Holm, 1994). Therefore fresh ovaries appear to be a better choice for oocyte size measurements and fecundity studies; however the majority of sampling takes place on board commercial vessels and these can normally provide only limited opportunities for analyses of fresh gonads which, along with the complexity of oocyte recruitment, mean that the fixation of samples is practically unavoidable.

The main advantage of histology is that it provides accurate criteria for classifying an individual oocyte into a stage type or category, particularly in the case of those that are atretic (Coward and Bromage, 2002) or in an interface between primary and secondary oocyte growth (Bucholtz et al., 2013). Therefore, despite implicit tissue shrinkage, gonad histology is a commonly used tool on a wide range of species. Paraffin was introduced as an embedding medium in the late 19th century and the main advantages are the low cost in use, the large diversity of staining methods developed, and that the sectioned portion of the embedding tissue can be large. In addition, paraffin is inert and does not interact chemically with the tissue, which is fundamental advantage in immunohistochemical studies (Verhoef et al., 2013). However, the substantial shrinkage of tissues in molten paraffin is unavoidable because of the warming process involved (Iwadare et al., 1984). The main advantages of resin as an embedding medium are the lesser degree of tissue deformation and shrinkage in comparison with paraffin (Dorph-Petersen et al., 2001) and the low temperatures at polymerization (Willbold and Witte, 2010).

We found that embedded paraffin oocytes of all stages had a lower mean diameter in comparison with those embedded in resin in the spawning albacore ovary. These results are in accordance with recent studies that compared the size of sardine (*Sardina pilchardus*) POFs (Ganias et al., 2007) and human adipocyte size (Verhoef et al., 2013) in the two embedding media. The differences in mean relative shrinkage of oocytes in paraffin in proportion to the shrinkage in resin became larger when the oocyte diameter, represented by OD_{Ni}, increased, reaching the maximum difference at oocytes in the HYD stage (with

Table 5
Mean fresh and embedded oocyte diameter (OD_{Ni}) for tertiary vitellogenic (Vtg3), germinal vesicle migration (GVM) and hydration (HYD) stage oocytes from Mediterranean albacore (*Thunnus alalunga*) ovaries collected in 2011. Differences in mean oocyte diameter (OD_{Ni}) between fresh oocyte measurements (OD_{fresh}) and the two embedding media (fresh vs. paraffin and fresh vs. resin) were expressed as percentages (Z), according to the formulas: $Z = 100 \times (x - y_1)\, x^{-1}$ and $Z = 100 \times (x - y_2)\, x^{-1}$, where x is OD_{fresh} and, y_1 and y_2 are $OD_{paraffin}$ and OD_{resin}, respectively. Differences in mean oocyte diameter between the two embedding media (paraffin vs. resin) were also reported: $Z = 100 \times (OD_{resin} - OD_{paraffin}) / OD_{resin}$.

Oocyte stage	n	Fresh	Resin	Paraffin	Fresh vs. Resin	Fresh vs. Paraffin	Resin vs. Paraffin
Vtg3	90	624 ± 18	515 ± 15	462 ± 23	17.5	26.0	10.3
GVM	90	690 ± 25	573 ± 19	513 ± 20	16.9	25.7	10.6
HYD	30	895 ± 35	658 ± 51	485 ± 32	26.5	45.8	26.2

n, number of oocytes measured.

Please cite this article as: Saber, S., et al., Stereological comparison of oocyte recruitment and batch fecundity estimates from paraffin and resin sections using spawning albac..., J. Sea Res. (2014), http://dx.doi.org/10.1016/j.seares.2014.05.003

Table 6
Mean oocyte packing density (OPD_i) for each oocyte stage according to the gonad subphase (advanced vitellogenic [AVT], migratory nucleus [MG] and, hydrated [HY]) in Mediterranean albacore (*Thunnus alalunga*) ovaries. Uncorrected refers when OPD_i was calculated using estimates of OD_{Vi} (uncorrected for shrinkage) and corrected refers when OPD_i was calculated using estimates of cOD_{Vi} (corrected for shrinkage). In terms of oocyte stages the abbreviations used are: primary growth (PG), cortical alveolar (CA), primary vitellogenic (Vtg1), secondary vitellogenic (Vtg2), tertiary vitellogenic (Vtg3), germinal vesicle migration (GVM) and, hydration (HYD).

		Uncorrected		Corrected	
		Resin	Paraffin	Resin	Paraffin
Gonad subphase	Oocyte	OPD_i (g^{-1}) ± SD	OPD_i (g^{-1}) ± SD	OPD_i (g^{-1}) ± SD	OPD_i (g^{-1}) ± SD
AVT	PG	153,985 ± 34,450	159,750 ± 26,812	45,469 ± 9969	46,327 ± 7766
	CA	5047 ± 1752	8634 ± 2122	2041 ± 705*	2923 ± 728*
	Vtg1	5165 ± 1024	8223 ± 3016	2376 ± 443	2971 ± 1076
	Vtg2	4495 ± 699	5541 ± 1269	2347 ± 348	2152 ± 480
	Vtg3	6605 ± 915	7920 ± 913	3711 ± 496	3205 ± 363
	Total (OPD)	175,298	190,069	55,945	57,579
MG	PG	144,229 ± 22,460	141,193 ± 34,689	43,234 ± 7207	41,315 ± 10,298
	CA	5470 ± 2911	9840 ± 2933	2270 ± 1201	3389 ± 1015
	Vtg1	4551 ± 1789	6208 ± 1679	2156 ± 819	2294 ± 614
	Vtg2	4003 ± 838	5183 ± 1580	2138 ± 427	2039 ± 626
	GVM	4208 ± 596	5097 ± 1139	2403 ± 327	2082 ± 460
	Total (OPD)	162,460	167,521	52,202	51,119
HY	PG	98,154 ± 36,355	108,053 ± 69,362	29,881 ± 11,072	31,113 ± 19,662
	CA	2901 ± 1120	4995 ± 2429	1194 ± 482	1720 ± 842
	Vtg1	3831 ± 907	5070 ± 2198	1769 ± 427	1853 ± 794
	Vtg2	5550 ± 1080	6261 ± 1353	2940 ± 578	2467 ± 523
	HYD	2500 ± 358	3753 ± 668	1024 ± 144*	644 ± 105*
	Total (OPD)	112,936	128,132	36,807	37,796

* Indicates values significantly different between resin and paraffin only for corrected estimates of OPD_i.

the 24%). As a result of this, lower estimations of volume fraction of these oocyte stages were found in paraffin when compared to resin and consequently the volume fraction of free space was higher in paraffin than in resin histological sections. Kraus et al. (2008) assumed that ovarian stroma shrinks proportionally to the average oocyte composition of the ovary, but our results showed that, although oocytes embedded in paraffin shrank more than in resin, the volume fraction of connective tissue in the resin histological sections was actually higher. One explanation for these higher values in resin might be due to the fact that the original connective tissue structure is better kept in place in resin, whereas in paraffin it 'loosens up' putting partly an explanation to the previously mentioned higher volume fraction of free space in paraffin. That is, morphology is better preserved in resin (Verhoef et al., 2013; Wittenburg et al., 2009).

Similar indications of differential shrinkage between fresh and embedded oocytes, depending on the oocyte stage and embedding medium, have appeared in contrasting two studies of cod ovaries. While shrinkage of late vitellogenic oocytes embedded in resin was about 7% (calculated from Kjesbu et al., 2011), in paraffin the shrinkage was 30 ± 9% (Kraus et al., 2008). Our results show that oocytes shrink due to the embedding process, with paraffin causing more shrinkage than resin, and that shrinkage of the oocytes in the HYD stage (45.78% in paraffin and 26.51% in resin, both in comparison with fresh oocytes) is higher than for other classes of oocytes such as those in the Vtg3 and GVM stages. Both albacore and cod produce pelagic eggs, and it is known that the water content in cod eggs is extremely high at about 93–98% (Jung, 2012; Thorsen et al., 1996) and, likely, comparable to that of albacore (Craik and Harvey, 1987). Although the estimation of the shrinkage of the oocytes in the HYD stage was performed using fresh oocyte measurements from only a single female, our results were very much similar to the figure of Kraus et al. (2008), who found that Baltic cod hydrated eggs shrank 48 ± 7%. Therefore non-uniform shrinkage occurs throughout oocyte development (Bucholtz et al., 2013; Kraus et al., 2008; Schismenou et al., 2012), i.e. presently as a function of stage *i* oocytes, and, as expected for the oocytes in the HYD stage will shrink more than the other oocyte stages in the dehydration phase of the histological processes (Schismenou et al., 2012). These results highlight the need to correct the diameters of the oocytes in the HYD stage separately from the rest of stage *i* oocytes.

As recommended by Lowerre-Barbieri et al. (2011) we used advanced histological/stereological quantification techniques represented by oocyte packing density (OPD) theory to better understand oocyte dynamics and to demonstrate the type of fecundity under question in the spawning ovaries of Mediterranean albacore. Oocytes of all stages were present in the examined ovaries pointing to an asynchronous oocyte development (Wallace and Selman, 1981). Two types of fecundity, determinate and indeterminate, have been defined in fishes according to the strategy of recruitment of oocytes to the stock of mature oocytes

Table 7
Estimates of mean batch fecundity (total number of oocytes) and relative batch fecundity (F_r) for Mediterranean albacore (*Thunnus alalunga*) (using merged nucleus migratory and hydrated gonad subphases). Uncorrected refers when OPD_i was calculated using estimates of OD_{Vi} (uncorrected for shrinkage) and corrected refers when OPD_i was calculated using estimates of cOD_{Vi} (corrected for shrinkage). Estimations are given in range and in mean ± SD.

	Batch fecundity (million of oocytes)		F_r (oocytes per gram of body mass)	
	Uncorrected	Corrected	Uncorrected	Corrected
Embedding medium	Range Mean ± SD	Range Mean ± SD	Range Mean ± SD	Range Mean ± SD
Resin	0.59–2.27 1.45 ± 0.49	0.24–1.24 0.72 ± 0.28	79–391 208 ± 81*	32–221 106 ± 54*
Paraffin	0.84–3.10 1.96 ± 0.73	0.14–1.27 0.56 ± 0.30	113–554 281 ± 123*	19–226 86 ± 61*

* Indicates values significantly different between uncorrected and corrected mean relative batch fecundity.

Please cite this article as: Saber, S., et al., Stereological comparison of oocyte recruitment and batch fecundity estimates from paraffin and resin sections using spawning albac..., J. Sea Res. (2014), http://dx.doi.org/10.1016/j.seares.2014.05.003

(Hunter et al., 1992). The common method of distinguishing between determinacy and indeterminacy is based on oocyte size distribution studies; species with determinate annual fecundity show a distinctive gap in the diameter frequency distribution between primary and secondary growth oocytes (Hunter and Macewicz, 1985; Murua et al., 2003). Conversely, species with indeterminate fecundity show an overlapping distribution of oocyte diameters in mature ovaries, although this evidence is not conclusive for determining the fecundity type (Murua and Saborido-Rey, 2003). Our results showed that the estimated number of primary growth stage oocytes per gram of ovary (OPD_{PG}) was very high in all gonad subphases; there is new (de novo) recruitment of oocytes from primary growth into vitellogenic stage oocytes. As expected for spawning individuals, a break in the oocyte size between Vtg2 stage oocyte and the MAGO in each gonad subphase separates the spawning batch from the standing stock of oocytes, this being most evident in ovaries in HY gonad subphase. Therefore the present results strongly suggest that the Mediterranean albacore has an indeterminate fecundity like is known for other tuna species (Otsu and Uchida, 1959; Schaefer, 2001).

Seven oocyte development stages in spawning Mediterranean albacore ovaries were distinguished based on their respective appearance. Commonly PG and CA oocyte stages in tuna species have been reported as one oocyte stage called 'unyolked oocytes' (Chen et al., 2010; Farley and Davis, 1998; Schaefer, 1996). According to oogenesis studies in bluefin tuna (*Thunnus thynnus*) cortical alveoli appears after the lipid droplets (Abascal and Medina, 2005; Sarasquete et al., 2002) and these have been reported to appear even after the yolk granules in seabass (*Dicentrarchus labrax*) (Mayer et al., 1988). For this reason, the term lipid-stage oocyte is used instead of cortical alveolar stage in studies of tuna species such as bluefin tuna and bigeye tuna (*Thunnus obesus*) (Aragón et al., 2010; Corriero et al., 2003; Figueiredo et al., 2008; Sarasquete et al., 2002). However, in our study we adopted the term CA to refer to the oocyte stage between PG and Vtg1 stages following the terminology of Brown-Peterson et al. (2011), as has been previously done with skipjack (*Katsuwonus pelamis*) (Grande et al., 2012).

According to Ganias (2013), the most important assumption in the use of OPD theory is that the fractional volume of the standing stock of vitellogenic oocytes should be high, i.e. the volume fraction of other follicles (previtellogenic and atretic follicles as well as POFs) and ovarian stroma should be relatively low. In this study, and in the study of Korta et al. (2010), the volume fraction of all stage *i* oocytes including those in PG stage were estimated. In addition, the volume fractions of atretic follicles, POFs, and connective tissue together with blood capillaries were presented along with the volume fraction of free space and lost oocytes in order to provide an accurate quantification of a series of volume fractions and so presenting a most detailed view of the spawning albacore ovary.

Fixation, tissue processing and staining, all produce tissue shrinkage which will influence the stereological estimation (Noorafshan et al., 2012). Statistical differences were found in the OPD estimates when using OD_{Vi} (based on $OD_{(ind)}$ uncorrected for shrinkage) and cOD_{Vi} (based on $OD_{(ind)}$ corrected for shrinkage) for all oocyte stages and for both embedding media. Moreover when comparing OD_{Vi}-based OPD_i in paraffin with those in resin, OPD_i results are overestimated in paraffin compared with those in resin, especially for the oocytes in the HYD stage. These results demonstrate why the oocyte shrinkage corrections are necessary in fecundity studies of this type. After the oocyte shrinkage corrections were applied the only significant differences in the estimates of OPD_i were found for CA (at AVT gonad subphase) and for the HYD oocyte stages. The explanation for these results seems to be found in the volume fraction of the oocytes, i.e. when V_{Vi} increased then OPD_i also increased and vice versa. Taken together, the present results showed that differences in HYD stage oocyte diameters causes differences in the volume fraction; OPD_i is primarily influenced by OD_{Vi} (and consequently by the $OD_{(ind)}$ measurements) and secondly by V_{Vi} (Kurita and Kjesbu, 2009). The theoretical OPD in ovaries of the spawning albacore was comparable with values seen in the ovary of spawning European hake (*Merluccius merluccius*) (Korta et al., 2010); in both species the estimated number of oocytes in the PG stage per gram of ovary (OPD_{PG}) was very high, and then the number of oocytes per gram of ovary decreased with OD_{Vi} (abruptly in the case of albacore ovaries) and slightly increased for the most advanced stage *i* oocytes in each gonad subphase.

Given that only ten females were used for fecundity estimations and natural variability in batch fecundity estimates is large (Chen et al., 2010), the aim of this study was not to provide estimates of batch fecundity but rather to compare the estimations reported by the two most commonly used embedding media. The F_r estimations were overestimated for both embedding media when using oocyte diameters that were uncorrected for shrinkage in the calculations, and the estimates in paraffin were higher than those in resin. However when oocyte diameters corrected for shrinkage were used, paraffin reported lower values of F_r than resin. Somewhat surprisingly, in spite of the higher degree of oocyte shrinkage in the GVM and HYD stages in paraffin, no significant differences in F_r were found between the two embedding media, suggesting that the OPD formula could equally well be used for batch fecundity estimations in paraffin as well as in resin. However, when F_r was estimated using only oocytes in the HYD stage, F_r was significant lower that when using only GVM stage oocytes for both embedding media. Similarly Schismenou et al. (2012) found that as a consequence of the high degree of shrinkage oocyte in the HYD stage, stereological methods for measuring batch fecundity based on ovaries in the HY subphase are less precise than using earlier oocyte stages. Oocytes in the hydration stage are present only for few hours in tuna ovaries, as well as in other species (Hunter et al., 1986; Schaefer, 2001; Schismenou et al., 2012). Commonly, oocytes in the GVM and HYD stages are both used to get F_r because of their advanced development they are easily distinguished from the other oocytes in the ovary and so reflect the batch soon to be spawned. The GVM stage oocytes appear to be better candidates for stereological batch fecundity estimations. However, it should be mentioned that if the purpose is restricted to estimating batch fecundity only instead of presenting a detailed picture of the formation of a batch of oocytes, then much simpler methodologies exist such as the 'Hydrated Oocyte Method'. In this quick method introduced several decades ago (see Hunter et al., 1985) these large oocytes are simply counted under the stereomicroscope and the number in each subsample is raised to the whole ovary and thereafter averaged.

5. Conclusions

In summary, the comparison of both embedding media showed that (1) non-uniform shrinkage occurs throughout the development of the various stage *i* oocytes, (2) mean oocyte diameters appear to be smaller in paraffin than in resin, (3) oocytes in the HYD stage shrink to a larger extent than oocytes in the other stages under consideration, with paraffin causing more shrinkage than resin, and (4) due to the high degree of shrinkage in the paraffin-based protocol, significant differences were found between the two embedding media in terms of volume fraction of 'free space' and connective tissue, showing that paraffin as an embedding medium distorts tissue morphology more than when resin is used for the same purpose, especially in the hydrated gonad subphase. The oocyte recruitment of spawning Mediterranean albacore follows the typical pattern of an asynchronous oocyte development and thereby shows an indeterminate fecundity. We document that OPD theory is a useful stereological tool to reveal this oocyte dynamic, including the numerical production of various types of oocytes, even the small PG stage oocytes. Furthermore, this study shows that oocyte shrinkage corrections must be used for accurate estimations including those of batch fecundity. When comparing paraffin and resin embedding media, after proper oocyte shrinkage corrections, (1) the only statistical differences in the OPD_i were found for oocytes in the CA stage (at the AVT gonad

Please cite this article as: Saber, S., et al., Stereological comparison of oocyte recruitment and batch fecundity estimates from paraffin and resin sections using spawning albac..., J. Sea Res. (2014), http://dx.doi.org/10.1016/j.seares.2014.05.003

subphase) and for HYD stage oocytes, (2) no statistical differences were detected in terms of relative batch fecundity, suggesting that in spite of the higher oocyte shrinkage, both paraffin and resin can properly be used in fecundity estimations, and (3) there was evidence of significant differences in relative batch fecundity estimations between germinal vesicle migration and hydration stage oocytes in both embedding media, indicating that GVM stage oocytes are better candidates for stereological batch fecundity estimations than the often seen, collapsed HYD stage oocytes.

Acknowledgments

We are very grateful to María José Gómez at IEO who has helped us with all sampling and laboratory work, to Nieves López and Javi Rey for their helpful suggestions. We also thank Bente Njøs Strand, Filipa da Silva, Anne Torsvik and Vemund Mangerud at IMR for their technical advice and to Anders Thorsen in the same laboratory for his advice on ImageJ. The collaboration with Federació Balear de Pesca i Casting, Federación Española de Pesca y Casting, the yacht clubs of S'Estanyol, Dénia, and Sóller, and with the fishing participants for providing the sample collection are greatly acknowledged. The IEO located in Palma de Mallorca is thanked for providing facilities during the sampling operation in Mallorca, as is Tim Dobinson for the English language proof reading of this paper and the two anonymous reviewers for the help with the revision. This work was mainly funded by a PhD grant by the IEO projects GPM-4 and GPM1213 to Sámar Saber.

References

Abascal, F.J., Medina, A., 2005. Ultrastructure of oogenesis in the bluefin tuna, *Thunnus thynnus*. J. Morphol. 264, 149–160.
Aragón, L., Aranda, G., Santos, A., Medina, A., 2010. Quantification of ovarian follicles in bluefin tuna *Thunnus thynnus* by two stereological methods. J. Fish Biol. 77, 719–730.
Boonstra, H., Oosterhuis, J.W., Oosterhuis, M., Fleuren, G.J., 1983. Cervical tissue shrinkage by formaldehyde fixation, paraffin wax embedding, section cutting and mounting. Pathol. Anat. Histopathol. 402, 195–201.
Brown-Peterson, N.J., Wyanski, D.M., Saborido-Rey, F., Macewicz, B.J., Lowerre-Barbieri, S. K., 2011. A standardized terminology for describing reproductive development in fishes. Mar. Coast. Fish.: Dyn. Manag. Ecosyst. Sci 3, 52–70.
Bucholtz, R.H., Tomkiewicz, J., Nyengaard, J.R., Andersen, J.B., 2013. Oogenesis, fecundity and condition of Baltic herring (*Clupea harengus* L.): a stereological study. Fish. Res. 145, 100–113.
Chen, K.-S., Crone, P.R., Hsu, C.-C., 2010. Reproductive biology of albacore *Thunnus alalunga*. J. Fish Biol. 77, 119–136.
Corriero, A., Desantis, S., Deflorio, M., Acone, F., Bridges, C.R., De la Serna, J.M., Megalofonou, P., De Metrio, G., 2003. Histological investigation on the ovarian cycle of the bluefin tuna in the western and central Mediterranean. J. Fish Biol. 63, 108–119.
Coward, K., Bromage, N.R., 2002. Quantification of ovarian condition in fish: a safer, more precise alternative to established methodology. Aquat. Living Resour. 15, 259–261.
Craik, J.C.A., Harvey, S.M., 1987. The causes of buoyancy in eggs of marine teleosts. J. Mar. Biol. Assoc. U. K. 67, 169–182.
Davis, T.L.O., 1982. Maturity and sexuality in barramundi, *Lates calcarifer* (Bloch), in the Northern Territory and south-eastern Gulf of Carpentaria. Aust. J. Mar. Freshwat. Res. 33, 529–545.
DeMartini, E.E., Fountain, R.K., 1981. Ovarian cycling frequency and batch fecundity in the queenfish, *Seriphus politus*: attributes representative of serial spawning fishes. Fish. Bull. 79, 547–560.
Dobrin, P.B., 1996. Effect of histologic preparation on the cross-sectional area of arterial rings. J. Surg. Res. 61, 413–415.
Dorph-Petersen, K.-A., Nyengaard, J.R., Gundersen, H.J.G., 2001. Tissue shrinkage and unbiased stereological estimation of particle number and size. J. Microsc. 204, 232–246.
Farley, J.H., Davis, T.L.O., 1998. Reproductive dynamics of southern bluefin tuna, *Thunnus maccoyii*. Fish. Bull. 96, 223–236.
Farley, J.H., Williams, A.J., Hoyle, S.D., Davies, C.R., Nicol, S.J., 2013. Reproductive dynamics and potential annual fecundity of South Pacific albacore tuna (*Thunnus alalunga*). PLoS One 8 (4), e60577. http://dx.doi.org/10.1371/journal.pone.0060577.
Figueiredo, M.B., Santos, A.G., Travassos, P., Torres-Silva, C.M., Hazin, F.H.V., Coeli, R., Magalahaes, B.R., 2008. Oocyte organization and ovary maturation of the bigeye tuna (*Thunnus obesus*) in the west tropical Atlantic Ocean. Collective Volume of Scientific Papers ICCAT, 62 (2), pp. 579–585.
Ganias, K., 2013. Determining the indeterminate: Evolving concepts and methods on the assessment of the fecundity pattern of fishes. Fish. Res. 138, 23–30.
Ganias, K., Nunes, C., Stratoudakis, Y., 2007. Degeneration of postovulatory follicles in the Iberian sardine *Sardina pilchardus*: structural changes and factors affecting resorption. Fish. Bull. 105, 131–139.
Grande, M., Murua, H., Zudaire, I., Korta, M., 2012. Oocyte development and fecundity type of the skipjack, *Katsuwonus pelamis*, in the Western Indian Ocean. J. Sea Res. 73, 117–125.
Howard, C.V., Reed, M.G., 2010. Unbiased Stereology. Three-Dimensional Measurement in Microscopy. QTP Publications, Liverpool,.
Hunter, J.R., Macewicz, B.J., 1985. Measurement of spawning frequency in multiple spawning fishes. In: Lasker, R. (Ed.), An Egg Production Method for Estimating Spawning Biomass of Pelagic Fish: Application to the Northern Anchovy, *Engraulis mordax*. NOAA Technical Report NMFS, 36, pp. 79–94.
Hunter, J.R., Lo, N.C.H., Leong, R.J.H., 1985. Batch fecundity in multiple spawning species. In: Lasker, R. (Ed.), An Egg Production Method for Estimating Spawning Biomass of Pelagic Fish: Application to the Northern Anchovy, *Engraulis mordax*. NOAA Technical Report NMFS, 36, pp. 67–77.
Hunter, J.R., Macewicz, B.J., Sibert, J.R., 1986. The spawning frequency of skipjack tuna, *Katsuwonus pelamis*, from the South Pacific. Fish. Bull. 84, 895–903.
Hunter, J.R., Macewicz, B.J., Lo, N.C.H., Kimbrell, C.A., 1992. Fecundity, spawning, and maturity of female Dover Sole, *Microstomus pacificus*, with an evaluation of assumptions and precision. Fish. Bull. 90, 101–128.
Iwadare, T., Mori, H., Ishiguro, K., Takeishi, M., 1984. Dimensional changes of tissue in the course of processing. J. Microsc. 136, 323–327.
Johnson, R.E., Sigman, J.D., Funk, G.F., Robinson, R.A., Hoffman, H.T., 1997. Quantification of surgical margin shrinkage in the oral cavity. Head Neck 19, 281–286.
Jung, K.-M., 2012. Theoretical and Experimental Studies of Atlantic Cod (*Gadus morhua* L.) Egg Buoyancy within a Metapopulation Framework. PhD dissertation University of Bergen,.
Kjesbu, O.S., 1991. A simple method for determining the maturity stages of northeast Arctic cod (*Gadus morhua* L.) by *in vitro* examination of oocytes. Sarsia 75, 335–338.
Kjesbu, O.S., Holm, J.C., 1994. Oocyte recruitment in first-time spawning Atlantic cod (*Gadus morhua*) in relation to feeding regime. Can. J. Fish. Aquat. Sci. 51, 1893–1898.
Kjesbu, O.S., Thorsen, A., Fonn, M., 2011. Quantification of primary and secondary oocyte production in Atlantic cod by simple oocyte packing density theory. Marine and Coastal Fisheries: Dynamics, Management, and Ecosystem Science 3, 92–105.
Korta, M., Murua, H., Kurita, Y., Kjesbu, O.S., 2010. How are the oocytes recruited in an indeterminate fish? Applications of stereological techniques along with advanced packing density theory on European hake (*Merluccius merluccius* L.). Fish. Res. 104, 56–63.
Kraus, G., Tomkiewicz, J., Diekmann, R., Köster, F.W., 2008. Seasonal prevalence and intensity of follicular atresia in Baltic cod *Gadus morhua callarias* L. J. Fish Biol. 72, 831–847.
Kurita, Y., Kjesbu, O.S., 2009. Fecundity estimation by oocyte packing density formulae in determinate and indeterminate spawners: theoretical considerations and applications. J. Sea Res. 61, 188–196.
Lowerre-Barbieri, S.K., Barbieri, L.R., 1993. A new method of oocyte separation and preservation for fish reproduction studies. Fish. Bull. 91, 165–170.
Lowerre-Barbieri, S.K., Brown-Peterson, N.J., Murua, H., Tomkiewicz, J., Wyanski, D.M., Saborido-Rey, F., 2011. Emerging issues and methodological advances in fisheries reproductive biology. Mar. Coast. Fish.: Dyn. Manag. Ecosyst. Sci 3, 32–51.
Mayer, I., Shackley, S.E., Ryland, J.S., 1988. Aspects of the reproductive biology of the bass, *Dicentrarchus labrax* L. I. An histological and histochemical study of oocyte maturation. J. Fish Biol. 33, 609–622.
McPherson, G.R., 1991. Reproductive biology of yellowfin tuna in the eastern Australian fishing zone, with special reference to the north-western Coral Sea. Aust. J. Mar. Freshwat. Res. 42, 465–477.
Murua, H., Saborido-Rey, F., 2003. Female reproductive strategies of marine fish species of the North Atlantic. J. Northwest Atl. Fish. Sci. 33, 23–31.
Murua, H., Kraus, G., Saborido-Rey, F., Witthames, P.R., Thorsen, A., Junquera, S., 2003. Procedures to estimate fecundity of marine fish species in relation to their reproductive strategy. J. Northwest Atl. Fish. Sci. 33, 33–54.
Noorafshan, A., Hoseini, L., Karbalay-Doust, S., Nadimi, E., 2012. A simple stereological method for estimating the number and the volume of the pancreatic beta cells. JOP 13, 427–432.
Otsu, T., Uchida, R.N., 1959. Sexual maturity and spawning of albacore in the Pacific Ocean. Fish. Bull. 59, 287–305.
Quester, R., Schröder, R., 1997. The shrinkage of the human brain stem during formalin fixation and embedding in paraffin. J. Neurosci. Methods 75, 81–89.
R Core Team, 2012. R: A Language and Environment for Statistical Computing. R Foundation for Statistical Computing, Vienna, Austria 3-900051-07-0, URL http://www.R-project.org/ [Available from http://www.R-project.org, accessed October 2012].
Ramon, D., Bartoo, N., 1997. The effects of formalin and freezing on ovaries of albacore, *Thunnus alalunga*. Fish. Bull. 95, 869–872.
Sarasquete, C., Cárdenas, S., González de Canales, M.L., Pascual, E., 2002. Oogenesis in the bluefin tuna, *Thunnus thynnus* L.: a histological and histochemical study. Histol. Histopathol. 17, 775–788.
Schaefer, K.M., 1996. Spawning time, frequency, and batch fecundity of yellowfin tuna, *Thunnus albacares*, near Clipperton Atoll in the eastern Pacific Ocean. Fish. Bull. 94, 98–112.
Schaefer, K.M., 1998. Reproductive biology of yellowfin tuna (*Thunnus albacares*) in the eastern Pacific Ocean. Inter-Am. Trop. Tuna Comm. Bull. 21, 205–272.
Schaefer, K.M., 2001. Reproductive biology of tunas. In: Block, B.A., Stevens, E.D. (Eds.), Tuna: Physiology, Ecology and Evolution. Academic Press, San Diego, California, pp. 225–270.
Scherle, W., 1970. A simple method for volumetry of organs in quantitative stereology. Mikroskopie 26, 57–60.
Schismenou, E., Somarakis, S., Thorsen, A., Kjesbu, O.S., 2012. Dynamics of de novo vitellogenesis in fish with indeterminate fecundity: an application of oocyte packing density theory to European anchovy, *Engraulis encrasicolus*. Mar. Biol. 159, 757–768.
Stéquert, B., Ramcharrun, B., 1995. La fécondité du listao (*Katsuwonus pelamis*) de l'ouest de l'océan Indien. Aquat. Living Resour. 8, 79–89.
Thorsen, A., Kjesbu, O.S., Fyhn, H.J., Solemdal, P., 1996. Physiological mechanisms of buoyancy in eggs from brackish water cod. J. Fish Biol. 48, 457–477.

Please cite this article as: Saber, S., et al., Stereological comparison of oocyte recruitment and batch fecundity estimates from paraffin and resin sections using spawning albac..., J. Sea Res. (2014), http://dx.doi.org/10.1016/j.seares.2014.05.003

Verhoef, S.P.M., Van Dijk, P., Westerterp, K.R., 2013. Relative shrinkage of adipocytes by paraffin in proportion to plastic embedding in human adipose tissue before and after weight loss. Obes. Res. Clin. Pract. 7, 8–13.
Wallace, R.A., Selman, K., 1981. Cellular and dynamic aspects of oocyte growth in teleost. Am. Zool. 21, 325–343.
Willbold, E., Witte, F., 2010. Histology and research at the hard tissue–implant interface using Technovit 9100 new embedding technique. Acta Biomater. 6, 4447–4455.
Wittenburg, G., Volkel, C., Mai, R., Lauer, G., 2009. Immunohistochemical comparison of differentiation markers on paraffin and plastic embedded human bone samples. J. Physiol. Pharmacol. 60, 43–49.
Witthames, P.R., Walker, M.G., 1987. An automated method for counting and sizing fish eggs. J. Fish Biol. 30, 225–235.
Zar, J.H., 1984. Biostatistical Analysis, 2nd ed. Prentice-Hall, London.

Please cite this article as: Saber, S., et al., Stereological comparison of oocyte recruitment and batch fecundity estimates from paraffin and resin sections using spawning albac..., J. Sea Res. (2014), http://dx.doi.org/10.1016/j.seares.2014.05.003